# Satellite Ultraquiet Isolation Technology Experiment (SUITE): Electromechanical Subsystems

Eric H. Anderson, Michael E. Evert,
Roger M. Glaese, James C. Goodding, Scott C. Pendleton
CSA Engineering, Inc.
2565 Leghorn Street
Mountain View, CA

Richard G. Cobb, R. Scott Erwin, Johnathan Jensen
Air Force Research Laboratory
Kirtland AFB, NM

Donald Camp, John Fumo, Marty Jessen
Trisys, Inc.
Phoenix, AZ

**SPIE Smart Structures and Materials 1999:
Industrial and Commercial
Applications of Smart Structures Technologies
Newport Beach, CA
March 1999**

# Report Documentation Page

*Form Approved*
*OMB No. 0704-0188*



| 1. REPORT DATE | 2. REPORT TYPE | 3. DATES COVERED |
|---|---|---|
| **MAR 1999** | | **00-00-1999 to 00-00-1999** |

| 4. TITLE AND SUBTITLE | 5a. CONTRACT NUMBER |
|---|---|
| **Satellite Ultraquiet Isolation Technology Experiment (SUITE): Electromechanical Subsystems** | 5b. GRANT NUMBER |
| | 5c. PROGRAM ELEMENT NUMBER |
| 6. AUTHOR(S) | 5d. PROJECT NUMBER |
| | 5e. TASK NUMBER |
| | 5f. WORK UNIT NUMBER |
| 7. PERFORMING ORGANIZATION NAME(S) AND ADDRESS(ES) **CSA Engineering,2565 Leghorn Street,Mountain View,CA,94043** | 8. PERFORMING ORGANIZATION REPORT NUMBER |
| 9. SPONSORING/MONITORING AGENCY NAME(S) AND ADDRESS(ES) | 10. SPONSOR/MONITOR'S ACRONYM(S) |
| | 11. SPONSOR/MONITOR'S REPORT NUMBER(S) |

12. DISTRIBUTION/AVAILABILITY STATEMENT
**Approved for public release; distribution unlimited**

13. SUPPLEMENTARY NOTES
**The original document contains color images.**

14. ABSTRACT
**see report**

15. SUBJECT TERMS

| 16. SECURITY CLASSIFICATION OF: | | | 17. LIMITATION OF ABSTRACT | 18. NUMBER OF PAGES | 19a. NAME OF RESPONSIBLE PERSON |
|---|---|---|---|---|---|
| a. REPORT **unclassified** | b. ABSTRACT **unclassified** | c. THIS PAGE **unclassified** | | **22** | |

# Satellite Ultraquiet Isolation Technology Experiment (SUITE): Electromechanical Subsystems

Eric H. Anderson* Michael E. Evert, Roger M. Glaese, James C. Goodding, and Scott C. Pendleton

CSA Engineering, Inc., 2565 Leghorn Street, Mountain View, CA 94043

Donald Camp, John Fumo, and Marty Jessen

Trisys, Inc., 21608 N. 20th Ave., Phoenix, AZ 85027

Richard G. Cobb, R. Scott Erwin, and Jonathan Jensen

Air Force Research Laboratory, Kirtland AFB, NM

## ABSTRACT

Spacecraft carry instruments and sensors that gather information from distant points, for example, from the Earth's surface several hundred kilometers away. Small vibrations on the spacecraft can reduce instrument effectiveness significantly. Vibration isolation systems are one means of minimizing the jitter of sensitive instruments. This paper describes one such system, the Satellite Ultraquiet Isolation Technology Experiment (SUITE). SUITE is a piezoelectric-based technology demonstration scheduled to fly in 2000 on PICOSat, a microsatellite fabricated by Surrey Satellite Technology, Ltd. Control from the ground station is planned for the first year after launch. SUITE draws on technology from previous research programs as well as a commercial piezoelectric vibration isolation system. The paper details the features of SUITE, with particular emphasis on the active hexapod assembly. A description of the PICOSat spacecraft and the other considerations preceding the development of the flight hardware begins the paper. Experiment goals are listed. The mechanical and electromechanical construction of the SUITE hexapod assembly is described, including the piezoelectric actuators, motion sensors, and electromagnetic actuators. The data control system is also described briefly, including the digital signal processor and spacecraft communication. The main features of the software used for real-time control and the supporting Matlab software used for control system development and data processing are summarized.

Keywords: Active vibration isolation, piezoelectrics, stable platform, microprecision control, satellite instruments

## 1. INTRODUCTION

The Satellite Ultraquiet Isolation Technology Experiment (SUITE) is an active vibration control system intended for the on-orbit stabilization of satellite instruments in the presence of low amplitude vibration or jitter. The outcome of this research was a specific set of physical hardware that will be orbited on a satellite called PICOSat.

Satellites and their instruments are subject to vibration throughout their lifetimes. Improving performance during the operational lifetime of satellites and instruments was of primary interest in this research. Although space is a much gentler vibration environment than that encountered during launch, vibration can cause problems during operation, the time over which the satellite functions on-orbit. Aside from their payloads, satellites require certain supporting equipment to carry out their missions. This may include reaction wheels to allow attitude control, solar array drives to position light gathering surfaces towards the sun, and cryogenic coolers to remove heat from instruments. The satellite may also act as host for multiple instruments, some of which may use gimbals or scanning/articulating components to make their measurements. All of these devices and others are sources of vibration.

The major consequence of vibration is degraded performance of various satellite instruments. For example, for a satellite camera used to image objects on the ground or in the Earth's atmosphere (Figure 1), a small vibration on the spacecraft may result in significant image degradation. A relatively minor 10 microradian (0.00057 degree) angular vibration or jitter is equivalent to 50 m in the field of view or image at a distance of 500 km. Some, but not all jitter-induced effects can be removed with signal and image processing. Actual reduction of the jitter by more direct means is often desirable, if it can be done efficiently. This physical jitter reduction augments what is done later in signal processing.

* Correspondence: Email eric.anderson@csaengineering.com WWW http://www.csaengineering.com; Voice (650)210-9000; Fax (650)210-9001

In addition to imagers or cameras, satellites contain other vibration-sensitive components such as inter-satellite communications links. Each particular type of component is more or less susceptible to vibrations in certain bandwidths, at certain amplitudes. This includes components that are actively pointed via gimbals or other devices, whose actuators do not have the bandwidth necessary to control the higher frequency vibration.

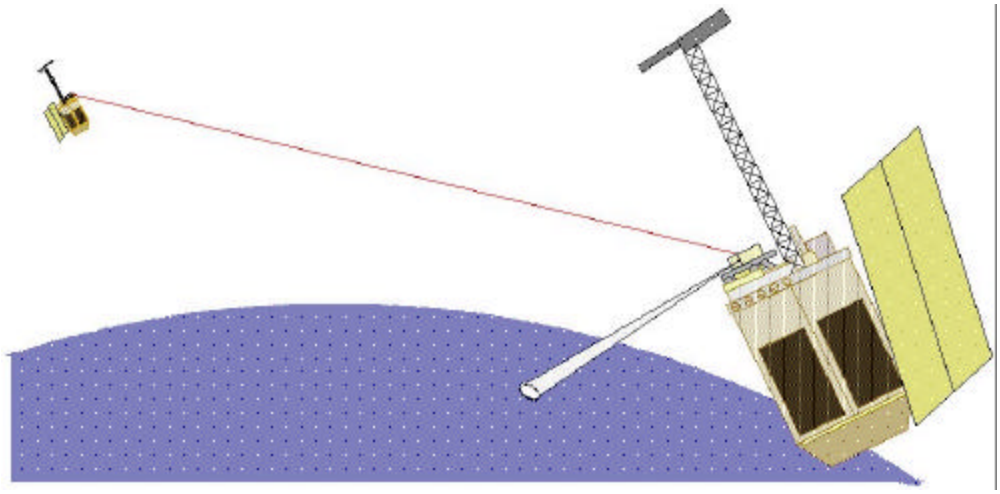

Figure 1: Stable platforms are required for jitter-free Earth observation and communication with other satellites

The diagram in Figure 2 shows the options for mitigating the effect of vibration on sensitive components. Other than a redesign of the vibration sources or the sensitive components, the options are three:

1. Vibration isolate the source of the disturbance
2. Modify the transmission of vibration through the satellite bus
3. Vibration isolate the sensitive component or payload

Of these approaches, the second requires access to and modification of the bus structure, while the first and third can be implemented as retrofittable solutions. There are advantages and practical limitations to each of these solutions. Isolation at the disturbance source is clearly a desirable approach. By blocking vibration transmission to the bus, all other components on the satellite are protected as well. But isolation of the disturbance is usually beyond the control of the instrument supplier, so this "noisy side" isolation may not be feasible in many circumstances. "Quiet side" isolation has the advantage of protecting the one critical component from all vibration sources on the spacecraft. Within the very serious constraints of added mass and cost, the supplier of the spacecraft instrument is free to build a vibration isolation system into his instrument mount or instrument-satellite mechanical interface.

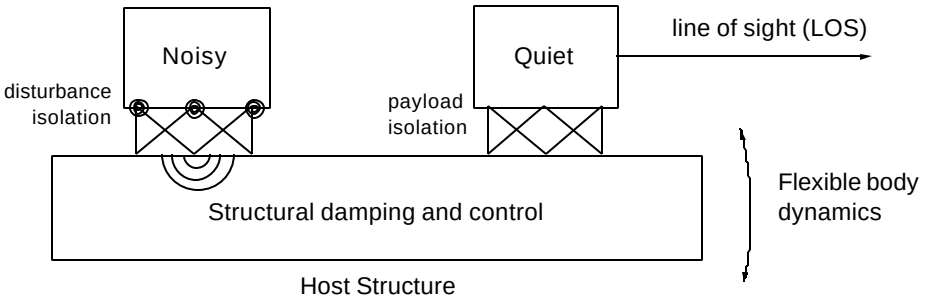


Figure 2 for mitigation of vibration on satellites

A quiet side isolation system certainly can be realized using passive components, i.e. those requiring no continuous input of power. A purely passive system will have limited performance, especially at lower frequencies. Two types of passive systems can be imagined depending on whether the isolation is deployed during launch. For a system that is deployed during launch, it must be expected to reduce the overall vibration, particularly the high frequency vibration experienced by the isolated component. It may be necessary to allow such a system to impact mechanical bumpers during the harshest part of launch. If the system is not deployed for launch, it must incorporate some type of release and deployment device. These will

add mass and some complexity to the system, but a deployment of a soft passive isolation system on-orbit is an attractive option, with benefits outweighing costs in many instances. Power is required only during deployment, not during operation.

The best passive vibration isolation system will be limited in performance by the constraints of physics and mechanical components. Thus, an active system, requiring power but delivering higher performance, can be considered. The possibility of such an active system for use in space has only recently become feasible with the advent of new electronic devices. An active vibration isolation system based on piezoelectric actuators was the focus of this research. A space flight system was built that will enable user-programmable active vibration isolation on an orbiting satellite.

SUITE is derived from an earlier effort that produced the UltraQuiet Platform (UQP).[1] It follows other technology demonstrations for vibration isolation on satellites including the cryocooler vibration control system flown on STRV-1b[2] and the Vibration Isolation Suppression and Steering (VISS)[3] system to fly on STRV-2. In comparison to VISS, SUITE has a narrower focus on vibration isolation, it uses a stiff passive mount with no launch locks, and it employs piezoelectric rather than electromagnetic actuators.

The paper continues with the following sections: PICOSat, Experiment Goals, System Architecture, Electromechanical Systems, Electronic Systems, Software and Firmware, Test Results, and Technology Applications.

## 2. PICOSAT

PICOSat is a micro-satellite procured by the U.S. Air Force Space Test Program (STP) with substantial funding from the DoD Foreign Comparative Test (FCT) program.[4] The satellite was manufactured by Surrey Satellite Technology Limited (SSTL) of Guildford, Surrey, England. Figure 3 shows a partially assembled PICOSat with the SUITE data control system (DCS) – second from the top in the stack of module trays - and the SUITE hexapod assembly (HXA) in the Earth Observing Compartment (EOC). The EOC walls, its Earth Observing Platform (EOP) cover, harnessing, solar arrays, stabilization boom, and other payloads are not integrated with the spacecraft in the photo. The fully assembled spacecraft has overall dimensions of approximately 690 × 360 × 360 mm, excluding the gravity gradient boom and any antennas on the EOP. In orbit the Earth would be at the top of this view. The HXA will be 'upside-down' with respect to the Earth.

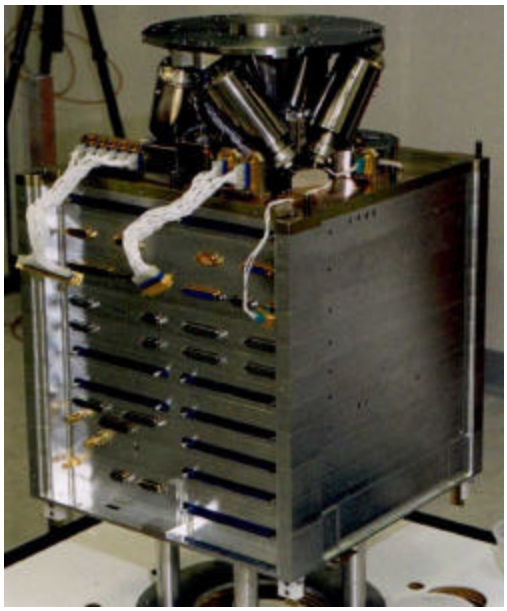

Figure 3: The PICOSat microsatellite shown with the SUITE DCS (second module tray from top of stack) and HXA (top) at SSTL during integration

The SSTL microsatellite platform, the Micro-Bus, was developed in 1988 and first flew in 1990. Since then, more than a dozen copies have been flown successfully, with each new satellite incorporating evolutionary improvements. The basic packaging concept is illustrated by Figure 3. A stack of modules or trays connected by tie-rods forms the structure of the satellite. The module trays contain circuit boards that provide for operation of the spacecraft or its payloads. The PICOSat is about 30% more massive than the standard Micro-Bus built by SSTL. SUITE contributes nearly one-fourth of the total satellite mass.

SUITE is one of four payloads or experiments on PICOSat. The others are: Coherent Electromagnetic Radio Tomography (CERTO), which is to determine ionospheric electron density using three-frequency beacon and fixed ground receivers; Ion

Occultation Experiment (IOX), which is to determine ionospheric electron profiles using GPS satellites; and Polymer Battery Experiment (PBEX), the first space demonstration of a polymer battery. SUITE interacts with the other payloads in its consumption of power – neither CERTO nor IOX can operate continuously with SUITE powered on. The only other major resource conflict relevant to SUITE involves sharing data download bandwidth with IOX.

Because the design of PICOSat was not complete at the start of this project, several satellite-payload integration issues were addressed during the research. The areas in which PICOSat constrained or drove the SUITE design most significantly were:

1. *Volume.* The PICOSat structure determined the overall volume allowed for SUITE and dictated the physical architecture used in the separate hexapod assembly (HXA) and data control system (DCS) hardware. In particular, the HXA was required to fit within the EOC, a space limited by shear panels, magnetic torque coils, RF antennas, and other structures. The approximate available space for the HXA, excluding these restrictions, was bounded by a volume $338 \times 338 \times 148.5$ mm. The DCS was required to fit within a standard module tray, with external dimensions $338 \times 338 \times 3.2$ mm.
2. *Mass and Inertia.* Since PICOSat was designed using rough estimates for the mass of SUITE, the total payload mass did not enter as a major constraint. However, since SUITE, especially the HXA, contributes significantly to the total spacecraft mass, it was desired to have the center of gravity (c.g.) of the HXA close to the physical x-y center of the spacecraft.
3. *Power.* PICOSat provides power at a non-standard voltage of 14 V. While at least one other payload is provided +14 V and +5 V power from PICOSat, it was decided that SUITE would operate on the single unregulated +14 V input. This meant an accommodation of the relatively low input voltage using carefully selected parts. The total power capacity of PICOSat (20-30 W) constrained the SUITE design and necessitated the use of low power components.
4. *Communications Bus.* PICOSat uses a Controller Area Network (CAN) bus for communication within the satellite. The CAN bus is a high-integrity serial data communications bus for real-time applications. It operates at data rates of up to 0.5 Megabits per second. CAN was originally developed in Europe for use in cars, and is now being used in many other industrial automation and control applications.
5. *Data Transfer Rates.* PICOSat does not provide high-speed data transfer to or from the spacecraft while it is in orbit. With limited line-of-sight contact from the ground station and inherent restrictions in on-board components, the estimated maximum data transfer rate was approximately 4 Mbytes per day.
6. *Electromagnetic Compatibility (EMC).* PICOSat has a redundant attitude control system (ACS) that begins with gravity gradient stabilization. The satellite makes use of sun sensors and magnetometers to provide attitude information and magnetic torque generators to provide attitude adjustment. The magnetic torque generators are a set of 3 or 4 wire coils that are actuated separately by a current that combines with the Earth's magnetic field to create a force to steer the satellite. For example, one magnetic torque generator coil is located in the EOC just above the HXA top lid. There was concern that the transducers in the SUITE HXA would be affected by the large local magnetic fields generated by the magnetic torque coils. More importantly, there was concern that various magnets and electrically-generated magnetic fields within SUITE would interfere with proper operation of the magnetometers. The main result for the design of HXA was the addition of extensive magnetic shielding.

## 3. EXPERIMENT GOALS

This section summarizes the goals of SUITE. These goals will be met ultimately in an on-orbit demonstration of capabilities during the 6-12 month PICOSat mission. The goals describe a series of benchmarks for achieving and recording vibration isolation. Because PICOSat is a small specialized spacecraft, sources of vibrational disturbances on the satellite are few. There are no reaction wheels, cryocoolers, or solar array drives, or articulating payloads aboard. The only two known events that will disturb the satellite are the deployment of the six-meter gravity gradient stabilization boom and the deployment of the antenna for another payload. Because the boom is critical to satellite operation and because it will be deployed before the satellite is fully operational, it is unlikely that SUITE itself will be functioning during that deployment. The antenna deployment offers a more feasible opportunity for demonstration of vibration isolation. However, there is a question concerning the available power should SUITE and the other payload be turned on simultaneously.

Because PICOSat presents an unusually quiet environment, SUITE was designed with the capacity to introduce disturbances to the spacecraft in a controlled manner. The experiment goals below assume the use of these disturbance generators.

### 3.1 Baseline Goals

The following two sections summarize the broadband and narrowband vibration isolation goals for quieting the SUITE payload in the presence of vibration on the satellite. The use of 'TBD' in the tables means that these values are to be filled in with experimental data when SUITE is operational.

**Broadband Vibration Isolation**

The vibration transmitted between the spacecraft bus and the isolated payload, measured as a root mean square quantity above 5 Hz, should be reduced in each of six axes by 20 dB (a factor of 10) in the presence of vibration sources located on the satellite. The upper limit to the frequency range of interest for the RMS calculation shall be determined by the measurement capability of the experiment, but shall reach at least 200 Hz. A reduction of less than 20 dB will be acceptable in one or more (but not all) axes depending on the absolute level of motion introduced into the satellite bus. The order of importance of the degrees of freedom for demonstrating vibration reduction is 1) the two rocking i.e. tilt (x and y rotation) modes, 2) the three translation modes, and 3) the twisting (or z rotation) mode. The z rotation degree-of-freedom is expected to be difficult to exercise because of the geometry constraints.

Table 1: Broadband satellite-payload vibration performance evaluation

| Degree of Freedom | Mode Description | Satellite RMS (5-200+ Hz) | Payload RMS (5-200+ Hz) | Ratio (Satellite to Payload) |
|---|---|---|---|---|
| X rotation | rocking or tilt | TBD μradian | TBD μradian | TBD (>20) dB |
| Y rotation | rocking or tilt | TBD μradian | TBD μradian | TBD (>20) dB |
| Z translation | bounce or plunge | TBD μm | TBD μm | TBD (>20) dB |
| X translation | lateral | TBD μm | TBD μm | TBD (>20) dB |
| Y translation | lateral | TBD μm | TBD μm | TBD (>20) dB |
| Z rotation | twisting | TBD μradian | TBD μradian | TBD (>20) dB |

**Narrowband Vibration Isolation**

The vibration transmitted between the spacecraft bus and the isolated payload, measured as the narrowband sinusoidal amplitude, shall be reduced in each of six axes by 30 dB (a factor of 31.6) or greater in the presence of vibration sources located on the satellite. Tests shall be conducted at three separate frequencies, nominally 5 Hz, 25 Hz, and 100 Hz. A reduction of less than 30 dB will be acceptable in one or more (but not all) axes depending on the absolute level of motion introduced into the satellite bus. The order of importance of the degrees of freedom for demonstrating vibration reduction is 1) the two rocking i.e. tilt (x and y rotation) modes, 2) the three translation modes, and 3) the twisting (or z rotation) mode.

Table 2: Narrowband satellite-payload vibration performance evaluation – low, mid, high frequency

| Degree of Freedom | Mode Description | Satellite 0-peak (5, 25, 100 Hz) | Payload 0-peak (5, 25, 100 Hz) | Ratio (Satellite to Payload) |
|---|---|---|---|---|
| X rotation | rocking or tilt | TBD μradian | TBD μradian | TBD (>30) dB |
| Y rotation | rocking or tilt | TBD μradian | TBD μradian | TBD (>30) dB |
| Z translation | bounce or plunge | TBD μm | TBD μm | TBD (>30) dB |
| X translation | lateral | TBD μm | TBD μm | TBD (>30) dB |
| Y translation | lateral | TBD μm | TBD μm | TBD (>30) dB |
| Z rotation | twisting | TBD μradian | TBD μradian | TBD (>30) dB |

### 3.2 Additional Goals

**Combined Broadband and Narrowband Isolation**

This set of criteria extends beyond the minimum set for the experiment. The performance goal is to achieve the results of Table 1 in combination with the results of Table 2.

**Narrowband Vibration Isolation from Payload-Attached Disturbance**

This criterion set is essentially the reverse of the set in Table 2. The vibration transmitted between the payload and the spacecraft bus, measured as the narrowband sinusoidal amplitude, shall be reduced in each of six axes by 20 dB (a factor of 10) or greater in the presence of vibration sources located on the payload. Tests shall be conducted at three separate frequencies, nominally 5 Hz, 25 Hz, and 100 Hz. A reduction of less than 20 dB will be acceptable in one or more (but not all) axes depending on the absolute level of motion introduced into the payload. The order of importance of the degrees of freedom for demonstrating vibration reduction is 1) the three rotation modes and 2) the three translation modes. Results for this set of criteria will be difficult to quantify because of the presence of the passive isolation system and the inability to deactivate it. Because of the anticipated effectiveness of the passive isolation system, a demonstration of 10 dB reduction of satellite vibration beyond that achieved with the passive system will be acceptable at 100 Hz.

**Narrowband Vibration Suppression of Payload-Attached Disturbance**

This criterion set is targeted to quiet the payload itself in response to vibration originating on the payload. The vibration on the payload, measured as the narrowband sinusoidal amplitude, shall be reduced in each of six axes by 20 dB (a factor of 10) or greater in the presence of vibration sources located on the payload. Reduction of the vibration transmitted between the payload and the spacecraft bus is not a goal, although it will be measured. Tests shall be conducted at three separate frequencies, nominally 5 Hz, 25 Hz, and 100 Hz. A reduction of less than 20 dB will be acceptable in one or more (but not all) axes depending on the absolute level of motion introduced into the payload. The order of importance of the degrees of freedom for demonstrating vibration reduction is 1) the two rocking or tilt (x and y rotation) modes, 2) the three translation modes, and 3) the twisting (or z rotation) mode.

**Other Possible Experiments**

- Vibration Reduction on the Payload Due to Uncontrolled Spacecraft Disturbances.
- Demonstration of Performance in Response to Oscillation of the Major Spacecraft Boom.
- Demonstration of Performance in Response to Tailored Disturbance Sources.
- Demonstration of Longevity of Experiment.
- Microprecision Pointing.
- Demonstration of Performance over a Wide Temperature Range.
- Broadband vibration isolation between the payload and satellite in the presence of payload-attached sources
- Broadband vibration suppression on the payload due to payload-attached sources
- Vibration suppression on the payload using the payload disturbance source as a control actuator

## 4. SYSTEM ARCHITECTURE

Meeting the goals of the previous section requires an active vibration isolation system. This section describes how active isolation is achieved in SUITE. The active isolation principle is presented. The approach to vibration isolation and strut-to-strut coupling in the hexapod configuration are discussed. The basic layout and connectivity of the subsystems is presented.

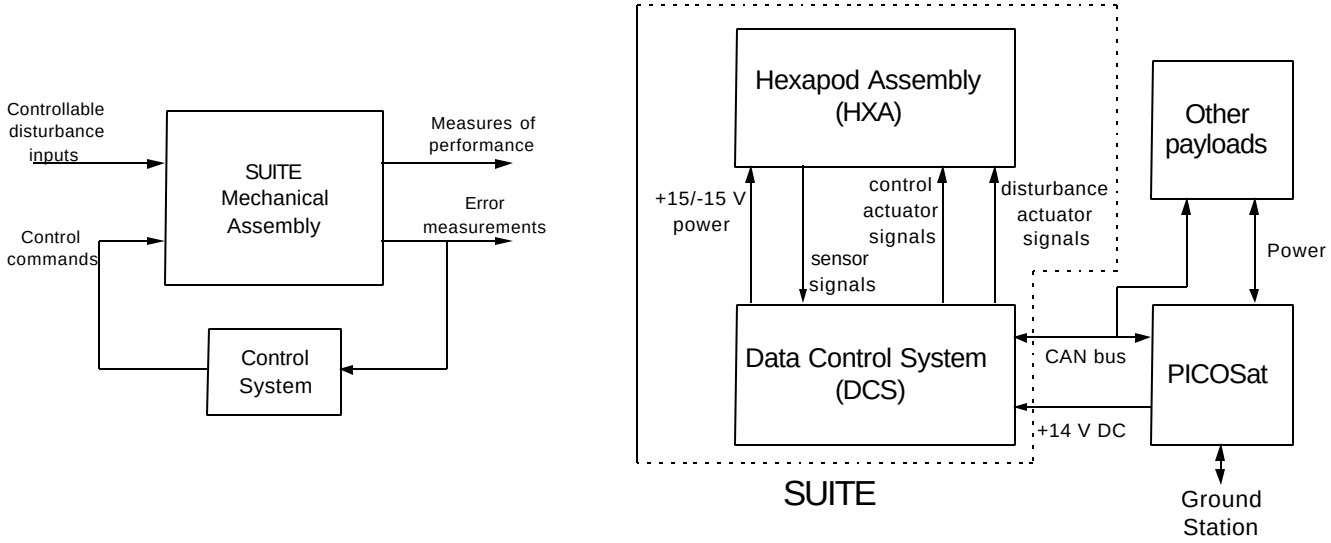


Figure 4: The basic architecture used for the experiment in vibration isolation and its relation to PICOSat

A series of experiments designed to meet the goals of the previous section required the architecture of Figure 4, as well as the means of modifying instructions remotely and means of storing and retrieving data. The realization of this experiment design and its relation to the PICOSat spacecraft are detailed on the right side of the figure. As the figure indicates, all interfaces with PICOSat are through the data control system (DCS). The DCS in turn provides power and transfers information to and from the hexapod assembly (HXA) and its actuators and sensors.

**Motivation – Vibration Isolation**

The SUITE design provides active vibration isolation in six axes, three translations and three rotations. Figure 5 illustrates these degrees of freedom on the SUITE HXA stick model. The active vibration isolation system complements a passive isolation system, which itself influences the same six suspension degrees of freedom. Although the mode shapes are indicated in the figure in simple terms, the asymmetry of the suspended payload and the geometrical orientation of the struts results in less well-defined mode shapes in the actual system, particularly in distinguishing between x and y translation and x and y rotation. SUITE does not deliberately employ a special hexapod geometry, such as a "cubic configuration" in order to decouple the influence of the active elements in each strut from the action of the other struts. Rather, the strut orientations were determined by the geometry imposed by the satellite. The particular geometry imposed by PICOSat is such that the z-direction isolation system stiffness is much greater than the stiffness in the x and y directions.

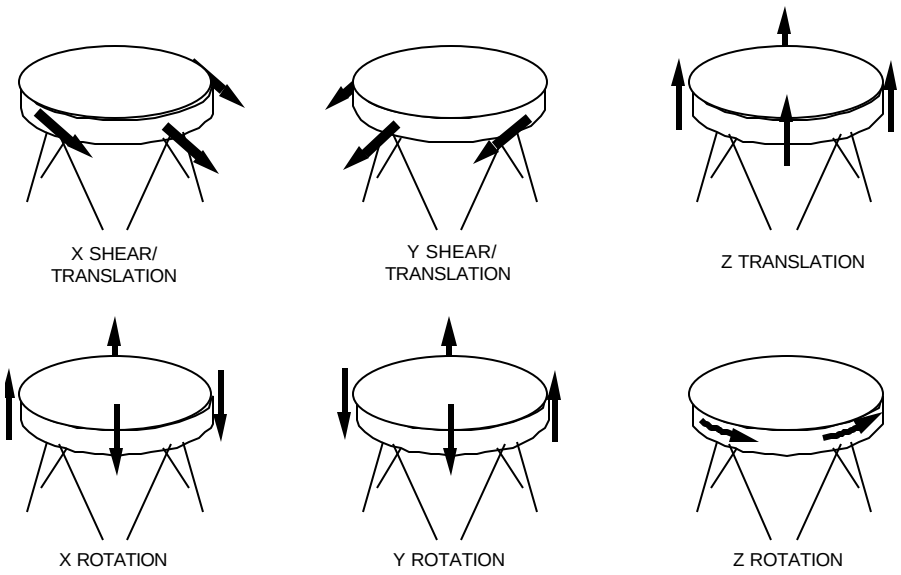


Figure 5: Six suspension modes are controlled by the active vibration isolation system

**Active Isolation Principle of Operation**

The six identical struts in the SUITE HXA achieve active vibration isolation through the use of stiff piezoelectric actuators that extend and contract in response to vibration originating at their base. The active portion of the system reduces vibration transmission at low frequencies and the passive portion attenuates high frequency inputs. It is useful to consider the architecture of a single strut to understand this. Figure 6 contrasts the approach used in SUITE with the more traditional "parallel" active-passive approach. In the parallel method shown in the figure on the left, a simple passive isolator (spring and dashpot) supporting a payload mass is augmented with a soft actuator in parallel mechanically, with almost no added stiffness. This actuator, usually a voice coil in practice, commands a force based on payload motion measurements, and possibly uses measured load information, to actively minimize vibration transmission.

The series approach described on the right adds an active stage below the passive isolator. In the diagram, this stage is represented by a stiff spring, $k_s$, and a force generator, F. The two-stage active-passive isolation system works in combination, and the active stage is designed with knowledge of the passive stage characteristics. The motion of the intermediate point, between the two stages, is measured and then actively nullified. This approach assumes that both the base and actuator are relatively rigid, such that with the active isolation turned off, the base motion and the intermediate point motion are the same. In practice, the base will not be entirely rigid, and compliance in the active stage results in an internal resonance that may limit control bandwidth. In contrast to the parallel architecture, the series architecture is designed to limit transmission from base to payload only. For suppression of vibration originating on the payload, it is necessary to augment the control with information from a payload motion sensor.

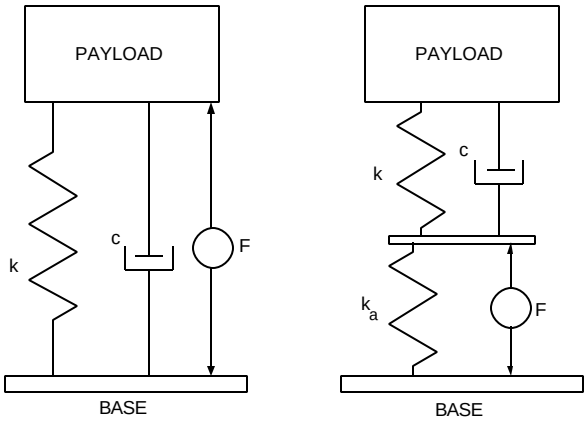


Figure 6: Parallel and series approaches to active enhancement of passive vibration isolation. SUITE uses the series approach.

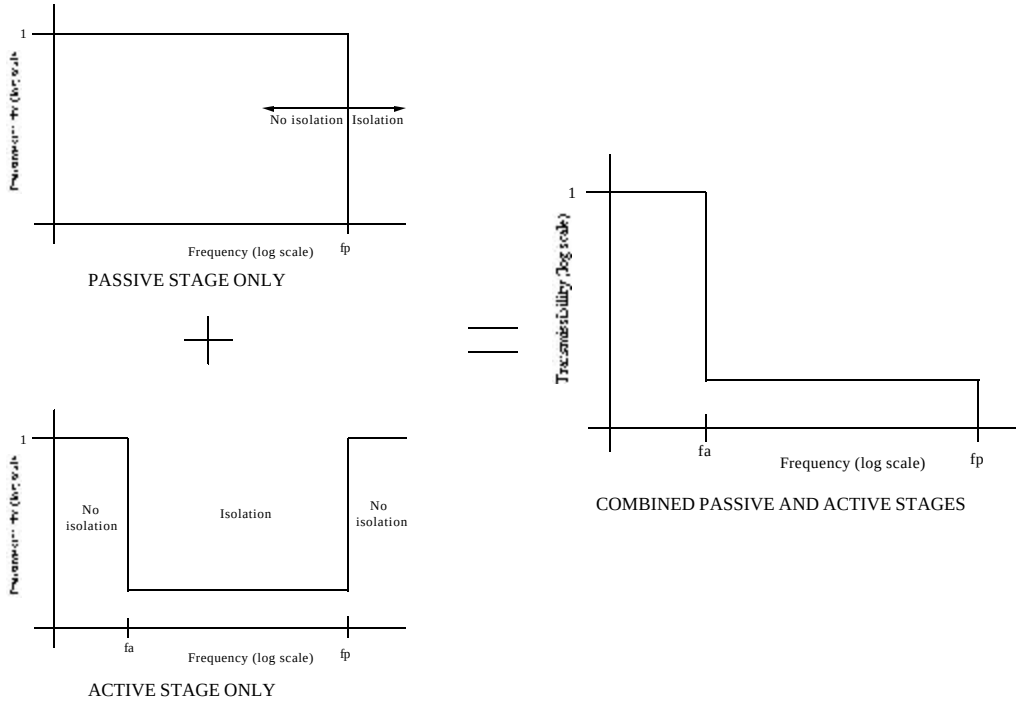


Figure 7: Idealized isolation transmissibility for series active-passive architecture

The SUITE system uses the series active-passive architecture. Without the active stage powered on, or with control gains of zero, the intermediate point within the strut moves with the base, but the passive stage still provides vibration isolation for the payload. The respective roles of the passive and active stages are illustrated by the single-axis transmissibility plots of Figure 7. In the three figures, a transmissibility of 1 means that the ratio of payload motion to base vibration is unity. The most significant idealizations for this single-axis case, are the lack of amplification at any frequency, and the perfect (zero) transmissibility at high frequency. The figure in the upper left shows the transmissibility with a perfect passive isolator. The isolation begins at the frequency $f_p$. The figure in the lower left shows the idealized transmissibility across an active stage. There is attenuation over the bandwidth of the active system, between the frequencies $f_a$ and $f_p$. The effect of a series combination of passive and active stages is illustrated with a graph on the right. The active system softens the isolator over the mid-frequency bandwidth, enhancing the passive transmissibility to reduce the isolation frequency of the overall system to $f_p$. The actual transmissibility modification in a hexapod support arrangement depends on the correct functioning of the six

struts. Together the modules modify the transmissibility in six axes. It is possible that effective isolation may be achieved in one axis but not in another, but the decoupled control used as a baseline does not consider the six suspension modes directly.

**SISO Active Vibration Isolation Architecture**

Each of the six isolation struts was designed to be identical with the others, both mechanically and electromechanically. The active-passive series architecture has been designed to decouple action of each strut from the others to allow a single input single output (SISO) control architecture. An example below illustrates the inherent decoupling resulting from this architecture.

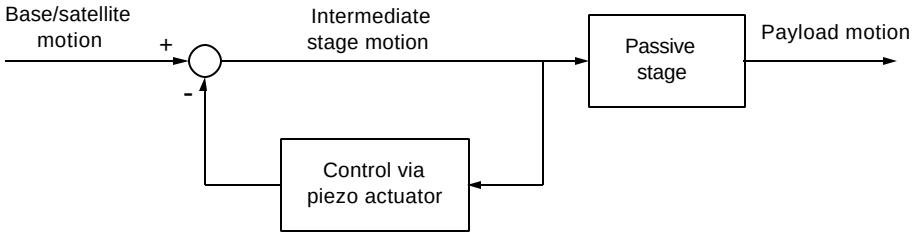


Figure 8: Block diagram of series active-passive isolation within each of the six struts

The SISO control approach is simple, requiring only a motion sensor and an actuator that can change its length within each strut. In Figure 8, there is base motion, perhaps due to satellite rotation, at the base of each strut that proceeds through to the intermediate stage. The motion of the intermediate stage is measured and fed through the controller, which in turn drives the piezoelectric actuators with the appropriate command to minimize the intermediate stage motion. The passive stage acts as a further, independent filter, modifying the transmissibility at high frequency. The control system has the ultimate goal of minimizing payload motion, so, lacking a payload motion sensor, it must act with some knowledge of the properties of the passive stage.

Although the control system is designed to be effective with a SISO architecture, there is coupling between separate legs in practice, particularly at the suspension mode frequencies. The coupling is illustrated by considering the lumped parameter model of a payload supported by two struts (Figure 9). This model is a linear approximation to the frequency-dependent passive stage impedance. Only two degrees of freedom – vertical translation and one rotation – are considered in this two-strut illustration. Finally, the base is assumed to be perfectly rigid. Parameters have been chosen to mimic the SUITE dynamics, including those of the geophone motion sensor (see Section 5).

During operation, a control input to actuator 1, indicated by the force, $f_1$, produces a motion $x_1$ at an intermediate point within strut 1, but also a motion $x_2$ within strut 2. The resonance near 1500 Hz is the local axial mode of the lower, active portion of the series mount. Above this frequency, there is reduced motion, $x_1$. The payload bounce and rocking modes at 28 and 44 Hz couple in weakly in this collocated transfer function. Because of the symmetry of this model, the same collocated transfer function would be expected at leg 2, i.e. $x_2/f_2 = x_1/f_1$. Even without the mounting symmetry, the collocated transfer function would be expected to show only a weak influence from the payload suspension modes.

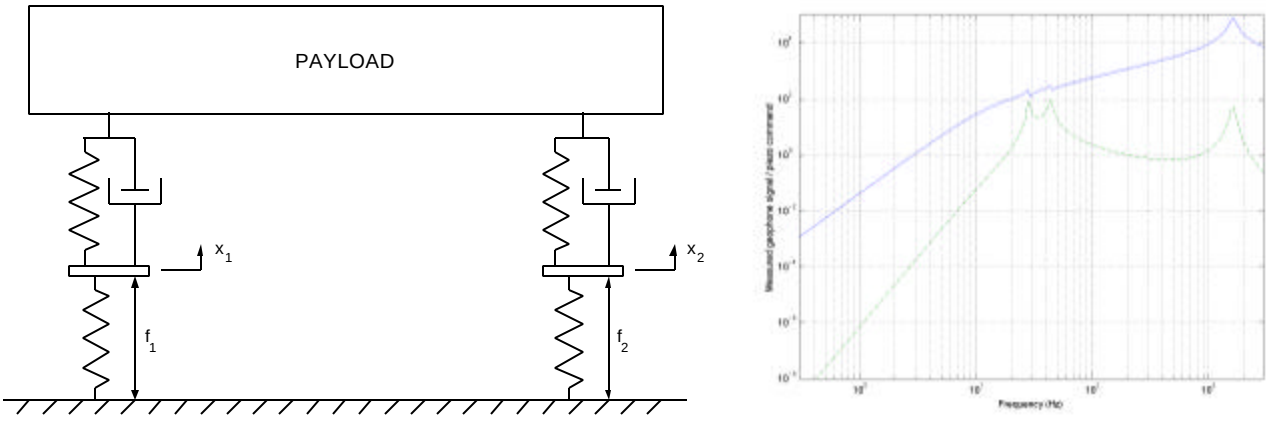


Figure 9: Model used to simulate dynamics and coupling of a two-strut isolation system; Magnitude of simulated plant transfer function, piezoelectric input to geophone output: collocated (solid) and noncollocated (dashed)

The heavily damped geophone resonance, in this case at 12 Hz, is apparent. The noncollocated transfer function, to the geophone in leg 2, from the piezoelectric actuator in leg 1, is reduced compared to the collocated transfer function. The noncollocated transfer function from the input command in leg 1 to the displacement in module 2 (or vice versa) is distinctly different from the collocated transfer function. In the transfer function $x_2/f_1$, little motion occurs at low frequency, as the passive stage springs deform to accommodate the piezoelectric extension. Coupling is strongest at the payload suspension frequencies. At higher frequencies, the response rolls off as the payload mass and inertia become difficult to translate and rotate. All of the deformation at high frequency occurs within the individual modules, and module-to-module coupling is minimized. The overall lack of coupling indicates that independent SISO control algorithms on each leg will be effective. However, as the lower stages are actively de-stiffened by the feedback, the largest amount of coupling occurs at lower frequencies, near the closed loop system suspension modes. This means that coupling could reduce achievable performance. Further, flexibility in the base structure, the satellite, also tends to couple the struts.

The SISO feedback control is the baseline, and therefore the system can be thought of as six decoupled systems of the type shown in Figure 10 operating simultaneously in parallel to minimize overall vibration transmission. The information flows from the strut through the controller, and eventually back to the strut. The nature of the various blocks of Figure 10 will become apparent in the next sections.

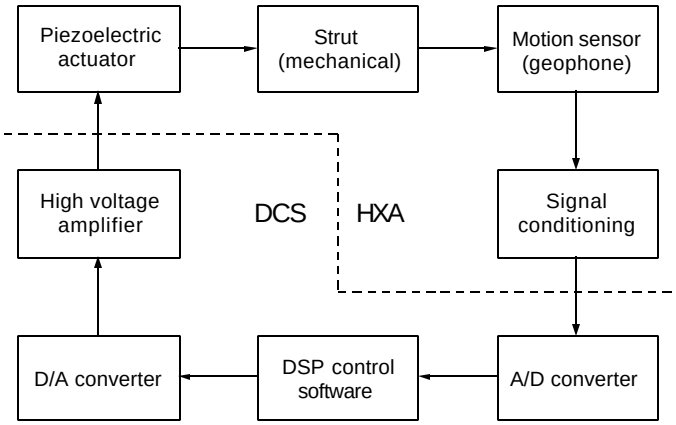


Figure 10: Functional block diagram of one SUITE active isolation module

Although the SISO collocated controller is baselined within each strut, SUITE has the built-in flexibility to allow complex, fully-coupled, 12-input, 6-output control architectures. Only software and the processing power of the digital signal processor (DSP) limit the architectures.

While the SISO architecture is effective for the nominal system, it will limit performance in the case of a strut active stage failure. If an actuator or sensor within one strut fails, or if the electrical connections to those transducers fail, the failure will be detected as part of the planned experiment sequence. Laboratory tests have shown that a failure of one strut, simulated by implementing a controller with zero gain, results in a loss of 85-90% of the overall active isolation system performance. Passive isolation system performance will not be affected. Upon detection of either a sensor failure or an actuator failure, it will become necessary to use the set of three motion sensors located on the isolated payload to augment a five-strut SISO control architecture. If only the strut sensor has failed, a 3-input, 1-output controller will be implemented using the actuator in the damaged strut. However, if the actuator has failed, it will become necessary to implement a multiple input multiple output control algorithm using eight (or nine) sensors and the five working actuators. Simulations show that over 90% of performance will be recovered. Failure of two struts will make control of six degrees of freedom difficult, particularly if the struts are adjacent to one another in the hexapod. Overall, the flexibility of the experiment will allow numerous options for software recovery from hardware component failures.

## 5. ELECTROMECHANICAL SUBSYSTEMS AND THE HEXAPOD ASSEMBLY

The hexapod assembly (HXA) refers to the entire hardware assembly located adjacent to the Earth observing Platform (EOP) of PICOSat. It includes the hexapod, i.e. the six struts supporting the SUITE payload, but it also includes various other components such as the vibration generators that contribute to the experiment. Major properties of the HXA are summarized in Table 3.

Table 3: Summary of HXA properties

| | |
|---|---|
| Total mass of HXA, including cables | 12.6 Kg |
| Strut attachment diameter (lower) | 213.7 mm |
| Strut attachment diameter (upper) | 196.8 mm |
| Mass of one strut | 0.332 Kg |
| Mass of one buzzer/PMA | 1.2 Kg |
| Mass of HXA suspended payload | 6.2 Kg |
| Maximum height | 139 mm |
| Maximum width (x and y directions) | 338 mm |
| Suspension frequencies | 25-75 Hz |

Figure 11 shows the hexapod assembly (HXA). The isolation system assembly is bolted to an aluminum base plate structure that serves as part of the satellite structure. The 12.0 mm (0.472 in.) thick base plate contains holes through which tie-rods are passed during satellite stacking and integration, and numerous tapped holes with locking heli-coil inserts into which other components were integrated. Material was removed selectively from the lower surface of the base plate to minimize mass while retaining stiffness and strength.

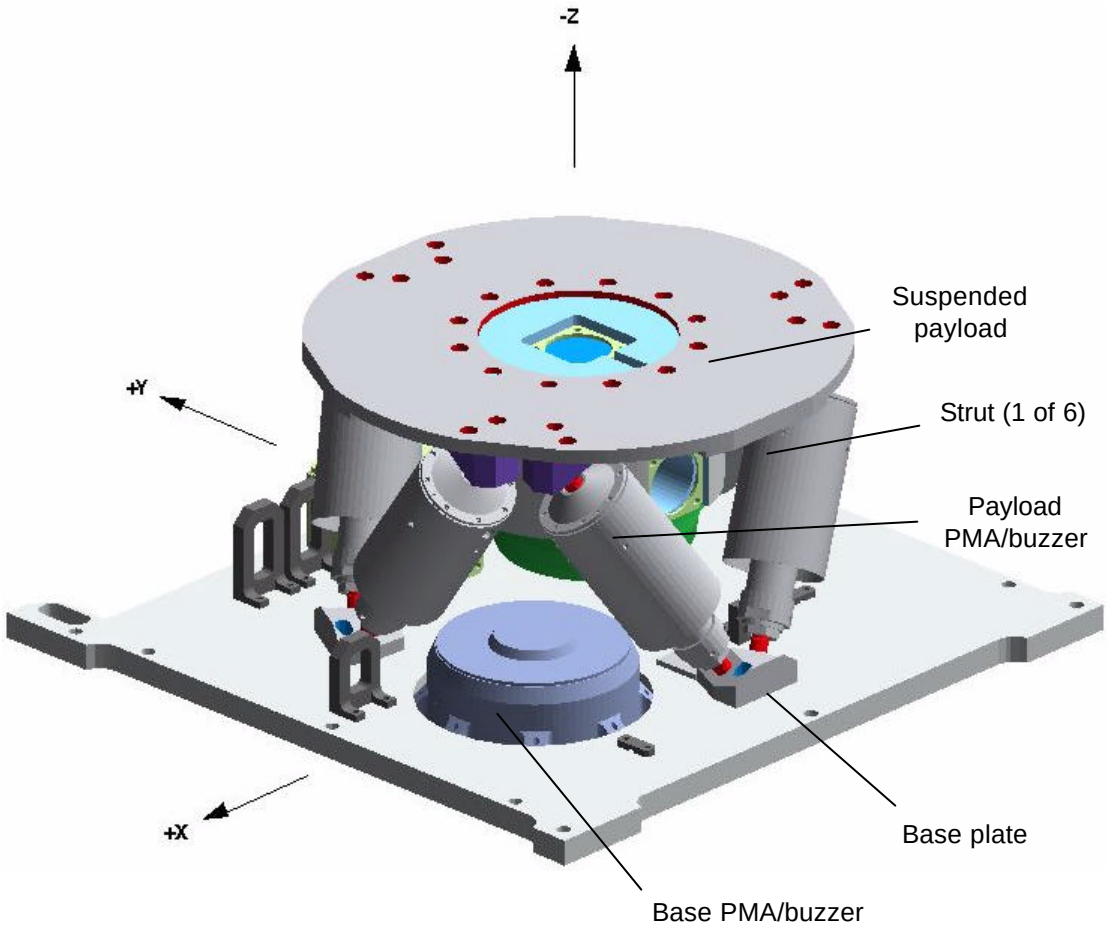


Figure 11: Hexapod assembly (HXA) showing local coordinate system

The six isolation struts attach to the base plate through three end fittings. At their upper (-z direction) ends the struts attach to the suspended payload via six end fittings. The payload consists of a 9.53 mm (0.375 in.) thick stainless steel lid and a core

assembly that is suspended from it in the +z direction to fill much of the central volume between the struts. The payload core includes a set of three geophone sensors measuring motion in the x, y and z directions, and a proof mass actuator (PMA) or buzzer. The payload buzzer acts at an angle of 5° with respect to the –z direction. An identical buzzer is inset 9.53 mm (0.375 in.) within the base plate. The base PMA acts in the z direction, approximately 180° from the direction of the payload buzzer. The base buzzer is capable of introducing significant vibration in the entire satellite. Barely visible in the figure, located on the +y portion of the plate, are three geophones that measure satellite or base motion. This tri-ax, when used in combination with the payload sensor tri-ax, provides a means of determining the effectiveness of the isolation system.

The wire harnesses that attach the HXA to the DCS come from below, at the +y edge of the base plate. (Figure 3 provides a clearer indication of this.) The harness connectors are attached at several bulkhead hard points and the cables are tied down with clamps. Several items are left out of the drawing of Figure 11. These are: Cables and harnesses, geophone truth sensors in the payload, magnetic shielding on the buzzers and top lid, launch limiting bumper system, strut cable clamps, and fasteners.

### 5.1 Strut Assembly

The hexapod contains six identical struts. The struts are intended to be the primary paths for load transmission to the isolated payload. Further, each strut (see Figure 12) is designed to be a single-axis member; that is, loads are transmitted along the axis of the strut but not in the other five axes. Therefore, modification of the transmissibility along the main axis of each of the six struts will modify overall hexapod transmissibility in six axes.

The two strut ends are designed to be incapable of transmitting moments. The remainder of the strut is a series of active and passive elements. From the bottom of the strut assembly, above the end flexure, a preload system insures that the piezoceramic device remains in compression throughout its lifetime. Upon application of the preload, the subassembly can be locked into place with radial set screws. The piezoelectric actuator is next in the strut stack. The section below discusses the actuator in greater detail. This is followed by the intermediate stage of the strut. The geophone motion sensor makes up the majority of the volume and mass of this section. The volume above the geophone is occupied by its signal conditioning board. The top subassembly consists of a passive isolation flexure, the motion limiters, and the upper end flexure.

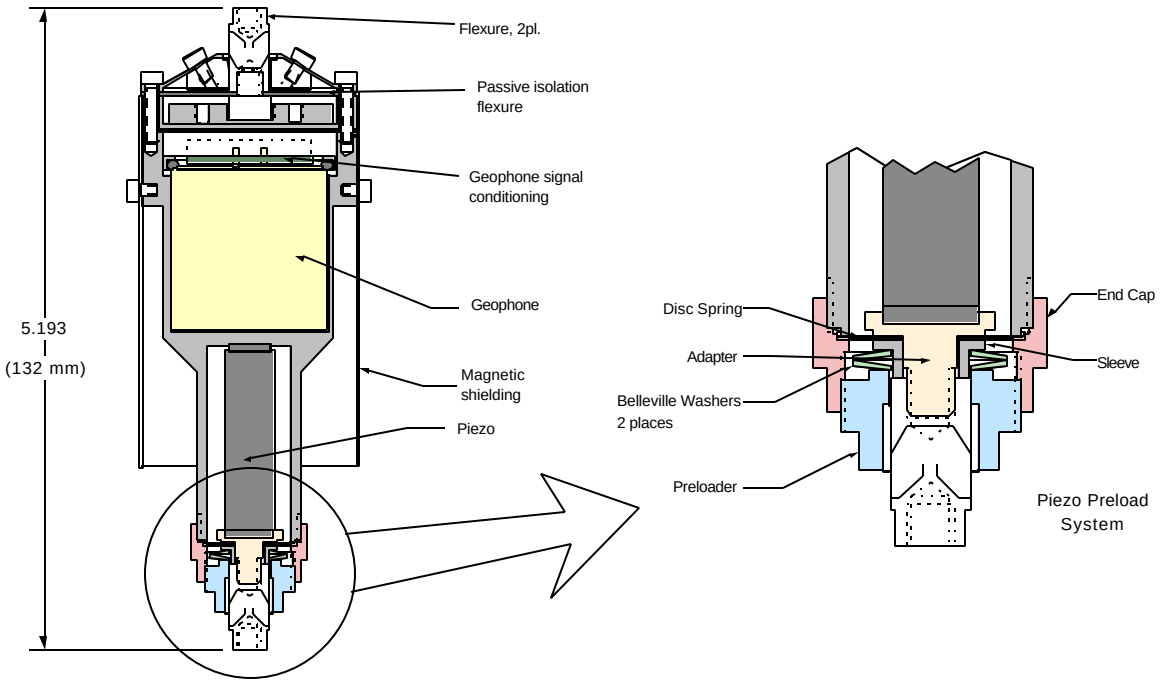


Figure 12: SUITE strut assembly

**End Flexures**

The purpose of the two end flexures is to reduce the transmission of loads in directions other than along the line of action of the strut. This is achieved through a cross-blade flexure arrangement that is soft in the two rotational directions. Previous isolation systems built by CSA have employed custom cross-blade flexures fabricated using a wire electrical discharge machining (EDM) process. The custom SUITE part has a nominal length of 17.50 mm. The flexures have a maximum

diameter of 8.0 mm and are tapped to accept fasteners. The blades are approximately 1.5 mm long and the gaps are 0.35 mm (14 mils) thick in the unloaded case. The flexures are designed so that when a load closes the gap, bottoming out the blade against the edge, the stresses are well below the level that would cause the material to yield. The nominal rotational stiffness is specified at 22 N-m/radian (0.38 N-m/degree).

**Piezoelectric Vibration Control Actuators**

Active vibration isolation is achieved when the piezoelectric actuator within each strut is deformed by the required amount. The actuator properties dictate the maximum amount of base or satellite motion that can be attenuated. There is one piezoelectric actuator per strut. The actuator must be extremely stiff so that it is able to enforce a specified displacement. The specific requirement most important in selecting an actuator for this application is its stroke capacity, because the amount of actuator stroke sets the amount of angular jitter that can be accommodated by the isolation system. In general, piezoelectric actuators are capable of at most 0.1% strain so that 10 μm of stroke can be achieved with a 10 mm tall stack. A 30 μm peak-peak stroke translates to ±1.25 milliradian for the HXA geometry. For the actuators used in SUITE, the relationship between deformation and voltage is approximately 0.30 μm/Volt.

The local vibration mode, in which the piezoelectric stack acts as a spring and the intermediate stage including the geophone as a mass, imposed a limit on the bandwidth of the series-type active isolation system. For effective control in the 150-250 Hz range, the frequency of the local mode should be well above 1 kHz, preferably above 1.5 kHz. Typical measured values in the SUITE struts were 1.5-1.8 kHz.

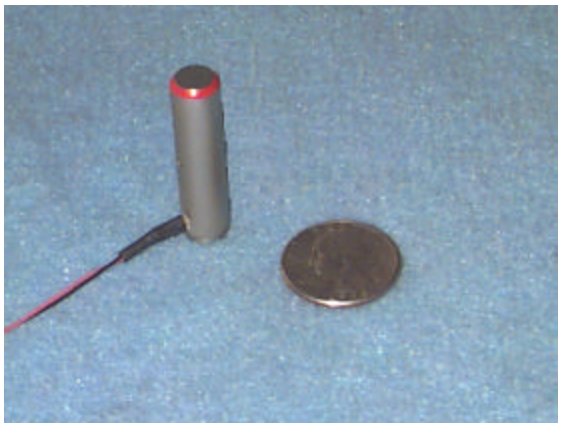

| | |
|---|---|
| Manufacturer | Physik Instrumente |
| Material | PZT |
| Acceptable voltage range | -20 V to +120 V |
| Operational voltage range | -15 V to +100 V |
| Operational stroke | 30 μm (1.18 mils) pk-pk |
| Dimensions | 9.50 × 40.00 mm ± 0.05 |
| Capacitance | 3.75 ± 5% |
| Temperature Range | -20°C to +80°C |
| Local in strut resonance frequency | > 1.5 kHz |

Figure 13: Piezoelectric stack actuator (with insulation and unterminated leads) and summary of characteristics

Figure 13 summarizes key features of the piezoceramic actuator and also shows the actuator with the two wire leads attached. Note that the stack is packaged in a stainless steel housing. Barely visible on the left side of the actuator is a 1.5 mm diameter vent hole. The purpose of this hole is to help equalize pressure during transition into the vacuum of space. A Belleville washer or spring set is used to preload the piezoelectric actuator.

**Motion Sensor Assembly**

The motion sensor located at the top of the active stage is the critical element in effecting the ultimate isolation performance, especially when the absolute motion is small. There is one geophone sensor per strut. The six geophones are the only error sensors used in the baseline feedback-only configuration. The primary requirements on the motion sensor were resolution, size, and cost. There are several possible sensors for use in an active isolation system of this type. These include accelerometers, geophones, and a variety of displacement sensors. Accelerometers capable of measuring low frequency, low level motion were prohibitively large and expensive for this product. Displacement is the preferred measurement quantity, but a compact low cost option was not available in the development timeframe. A geophone was therefore baselined as the motion sensor. Geophones are inertial sensors with a long history of use in measurement of seismic motion. Their sensitivity-to-noise ratio at low frequencies, between 1 and 10 Hz, is often superior to that of accelerometers.

The primary design variables in a geophone are the responsivity and the suspension frequency, i. e. the natural frequency of the moving mass on the spring. The total internal stroke of the moving mass is a secondary design variable. The responsivity is expressed in units of voltage/velocity (e. g. V/m/s or V/in/s). It indicates the signal amplitude generated for a given velocity and characterizes a sensor above the suspension frequency. The suspension frequency is the quantity of greater interest in the SUITE design. The geophone is only strictly a velocity sensor above this suspension frequency. Below its suspension frequency, the geophone acts as a sensor of the second time derivative of velocity, also known as jerk. In the frequency range of its resonance, the sensor output transitions from jerk to velocity. Figure 14 highlights the value in

decreasing the sensor suspension frequency. For good performance this suspension frequency should be made as low as possible.

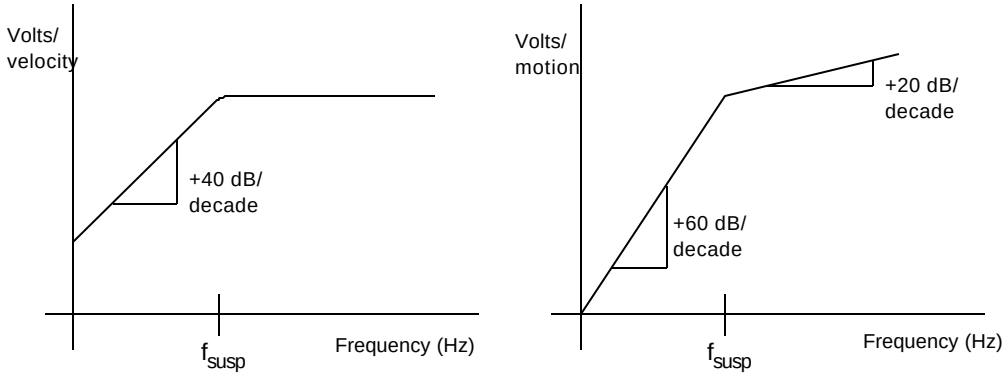


Figure 14: Geophone output responsivity per input velocity and displacement

Within the constraints of the SUITE strut geometry, a 4.5 Hz suspension frequency geophone was the softest possible in an acceptable package size. A 12 Hz sensor was used in the struts because sensors with lower suspension frequencies can be used in only one direction with respect to gravity.

One custom GS-11D geophone manufactured by Geospace Corp. of Houston, TX is used in each strut. Properties of this sensor are summarized in Figure 15. This particular custom geophone is designed to work at angles of 30-90° with respect to the action of gravity. The zero-g environment of space is equivalent to a 90° orientation on the ground. With the struts at an angle of 55° (35° with respect to gravity), the orientation just fits within the allowable range. The geophone is held securely in place by a mechanical subassembly (see Figure 12).

The 12 Hz suspension frequency results in a 1.7 mm sag in a 1-g field (1.4 mm at the 55° strut angle) and will result in 10 mm sag in a typical 6-g launch load case. It is expected that the internal mass will therefore bottom out during launch. However, as the '30/90' description implies, the omnidirectionality is not an official specification. Each geophone was modified with a vent hole to avoid rapid decompression in a vacuum. Geophones are in general extremely rugged devices that are difficult to damage. They were tested to 15 g RMS.

| | |
|---|---|
| Manufacturer | Geospace Corp. |
| Part Designation | GS-11D 30/90 10360 |
| Responsivity | 0.10 V/mm/s (2.54 V/in/s) |
| Suspension frequency | 12 Hz |
| Moving mass | 16 g |
| Resistance | 4000 Ohms |
| Dimensions | 1.32 in high (+ 0.135 in terminals) × 1.25 in OD |
| Total mass | 125 g (4.4 oz) |
| Operating and storage temperature | -50°C to +100°C |

Figure 15: Geophone motion sensor and signal conditioning board and summary of sensor characteristics

**Sensor Conditioning**

The signal generated by the geophone at typical satellite motion amplitudes is in the range of several millivolts, a level inadequate for noise immunity or meaningful control. A high gain amplifier stage was therefore required. The signal conditioning stage should be located as near as possible to the geophone sensor to minimize the amplification of noise picked up on the line transferring the signal from the sensor package to the A/D converter. Therefore it was decided to mount the conditioner directly to the geophone transducer inside each strut. In contrast to previous implementations, the signal conditioning was of a differential rather than single-ended type to guard against EMI and increase common mode rejection in the uncertain EMI environment of PICOSat. Figure 15 shows a typical geophone signal conditioning circuit. The circuit

board is soldered directly to the geophone for use. The circuit board fits within the outer diameter of the geophone, allowing for a thin clamping ring to hold the geophone in place. The operational amplifier used in the signal conditioning stage, not the transducer itself, is the principal contributor to the total noise output from the sensor assembly. The practical effect of this noise is a limitation on the low frequency sensor resolution and therefore the lower end of the bandwidth of the active isolation system. Further details describing the design considerations for op-amp geophone conditioning are provided elsewhere.[5] The mating wire assembly, including the high and low signal lines, three power lines, and mechanical strain relief line, are all soldered to the board. During installation, the geophone signal conditioning is potted to provide protection for the board and strain relief for the five wires that attach to it. The wires exit through a small hole on the side of the strut. The low power Burr-Brown INA-118 instrumentation amplifier with a gain of 500 forms the conditioning core. In operation, the overall signal conditioning draws 9-11 mA per rail (-15V and +15V) per circuit board, for a total power of about 0.3 W per strut.

**Passive Isolation Stage**

Each strut contains a passive isolation stage that will isolate the payload regardless of the state of the active system. The stage in each strut combines with the stages in the other struts to minimize transmission of high frequency satellite motion to the isolated payload.

From the initiation of the project, the preference was to use elastomeric materials in some form. Constraints on the passive isolators included

- Physical volume limitations with the struts (diameter and height)
- A desire to minimize outgassing through proper materials specification
- Stiffness and damping properties
- Preference for a linear stiffness element
- The need to protect the system with minimum height from vibrations during launch

Previous isolation systems built by CSA have made use of elastomers in one of two ways. Either the material is used in bulk, providing both the stiffness and damping properties of the isolator, or it is used primarily to dissipate energy as a lossy element while stiffness is provided with a separate metallic component. The low mass of the SUITE HXA payload steered the design towards a damped flexure type system in which the compliance could be increased and the response made to stay linear in one-g or zero-g environments.

The limited diameter drove the design to incorporate spiral elements in order to extend the effective length of the bending elements and thus increase compliance and improve linearity. The constraints on outgassing were gradually relaxed as details on integration with PICOSat were discussed. It became apparent that none of the payloads on this small satellite was dependent on optics with extreme sensitivity to contaminants. Nevertheless, the passive stage was designed with a material and a geometry to minimize total outgassing.

The desired suspension frequencies for the HXA were between 30 and 60 Hz. However, the geometry of the Earth Observing Compartment on PICOSat was such that the HXA became preferentially stiff in the z or plunge (bounce) direction. The separation between the lowest and highest suspension frequencies was expected to be closer to 2 (Table 4). Therefore, the lowest frequency modes (x and y translation) were designed to occur at approximately 30 Hz. The damping of the passive stage was intended to result in dynamic amplifications at resonance of between 5 and 10 times, i.e. $5 < Q < 10$. This is a compromise between the amplification at resonance and the rate of transmissibility rolloff above the suspension resonances. Too large a Q tends to increase the burden on the active system, since it must effectively provide a notch in the transmissibility to counter the amplifications at the suspension resonances.

Although the HXA is expected to experience small motions on orbit, it was still preferred to have a linear compliance element for the passive stage. The linearity makes analysis easier and more direct in terms of computation of stresses and deflections. It also provides for greater consistency between the one-g and zero-g tests.

The passive isolation system could have been designed to carry full launch loads and therefore to isolate the hexapod assembly from the rough loads of launch. However, there is no great need to protect the particular SUITE HXA payload. Instead, the launch constraint becomes one of survivability. At a minimum, the passive isolation system needs only to survive launch and then deliver nominal performance on orbit. In this case a philosophy of motion limiting was used so that the largest launch loads do not pass through the passive isolators.

Figure 16: Struts during assembly prior to integration of passive isolation stage

Table 4: Summary of predicted passive suspension frequencies

| Mode | Frequency |
|---|---|
| Shear mode (Y translation) | 27.8 Hz |
| Shear mode (X translation) | 28.0 Hz |
| Payload buzzer suspension | 31.4 Hz |
| Satellite buzzer suspension | 32.0 Hz |
| Twist (Z axis rotation) | 50.8 Hz |
| Bounce (Z axis plunge) | 59.6 Hz |
| Tilt mode 1 | 68.8 Hz |
| Tilt mode 2 | 70.0 Hz |

Finite element models were developed to study flexure stiffness, linearity, and stress distributions under load cases simulating launch. The resulting design, a sandwich flexure consists of a 22 mil layer of Beryllium-Copper, a 2 mil viscoelastic, and a 3 mil constraining layer of Beryllium-Copper. The material loss factor was chosen to provide a Q of 8-10 in the suspension modes in the 10-30°C range. The flexures are visible in Figure 16.

During vibration testing, multiple damped flexures failed at high stress locations. This drove the enhancement of the internal motion limiting within the passive stage (top of struts in Figure 16) and the addition of external HXA bumpering. The internal motion limiters prevent flexure motion that would result in stresses exceeding material yield. The external motion limiting system acts to restrain motion in the z direction by C-brackets that surround three lips emerging from the outer diameter of the payload. The system limits rotations and lateral motion by means of a ring surrounding the payload. In each case a Delrin liner forms the protective layer in front of an aluminum backing structure.

### 5.2 Truth Motion Sensors

There are six other geophone motion sensors used in the HXA in addition to the six located in the struts, three on the base plate and three embedded in the payload. Each of the six sensors measures motion in the negative direction (i.e. –X, -Y, and –Z). The Z-direction sensors are of the same type as the strut motion sensors, with a 12 Hz suspension frequency. The four X and Y direction sensors have a 4.5 Hz suspension frequency. They are designed to work perpendicular to the Earth's gravity field, or, alternatively, in zero-g. The signal conditioning is identical to that used for the strut sensors.

### 5.3 PMAs Disturbance Generators

As noted elsewhere, it was necessary to incorporate controllable disturbance sources within SUITE. This is accomplished by two identical electromagnetic proof mass actuators (PMAs). A mass suspended on a spring is driven by an electromagnetic actuator that receives a command signal from the DCS. One PMA is attached to the base plate. It is capable of introducing forces directly into the satellite in the z direction. The other device is mounted on the hexapod payload. The devices (Figures 17 and 18) incorporate a double magnetic coil and dual flexures. The mass is allowed to rotate slightly as it moves. Overall motion is limited to 0.100 inches peak-peak. This bumpering limits motion primarily at low frequency. The PMAs were tested separately for launch survival to 16 g RMS vibration levels. Force output is 4.5 lb/Amp. With a limit of ±15 V, a resistance of 62 Ω, and an inductance of 13 mH, the maximum force on station is just over 1 lb. The PMAs can be driven up to 100 Hz. The bandwidth is restricted by the speed of the microcontroller used to generate the PWM drive signals. Arbitrary 128-point drive records, limited to 8 bits can be generated by the DSP for output through the PWM amplifiers to the shakers. In tests, a 1-50 Hz chirp is a typical output drive signal.

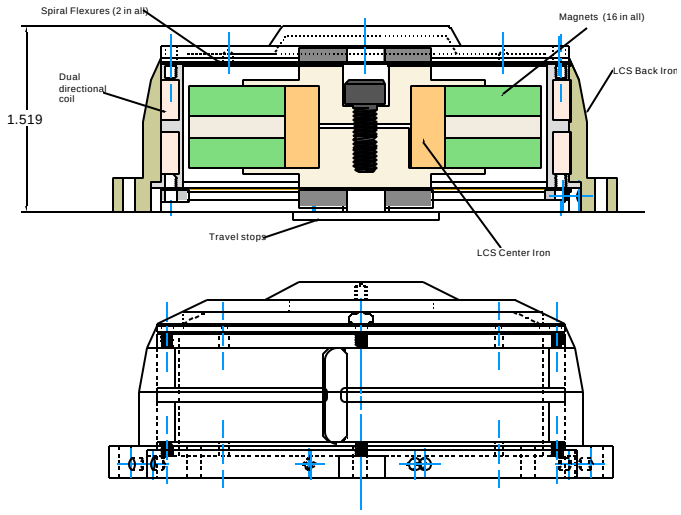


Figure 17: Cross-section of proof mass actuator vibration generators used on base and payload

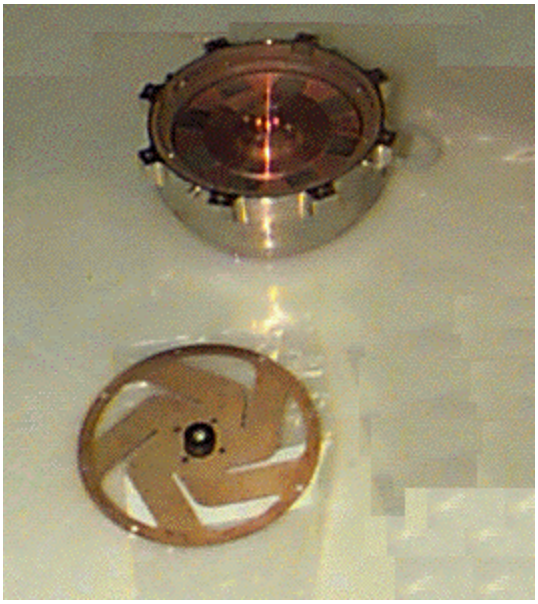

Figure 18: Vibration generator (PMA) shown from under side and the spiral flexure used in the PMA

### 5.4 Magnetic Shielding

Issues of electromagnetic compatibility drove several aspects of the HXA design. The magnetic components – the PMAs and the geophones – produce DC and AC magnetic fields beyond their physical housings (Figure 19). The geophone magnetic circuit is especially leaky. The AC leakage concern was greater from the PMA. PICOSat has magnetometers located less than 100 mm from some of the magnetic elements of the SUITE HXA. In order to minimize transmission of magnetic fields to the magnetometer locations, high permeability "mu-metal" shielding was used extensively in the HXA. Each geophone and each PMA was enclosed or nearly enclosed in the material. The cylindrical shape of the struts is due largely to the magnetic shielding "lampshade." In all, the dense shielding structures added approximately 0.5 Kg to the HXA.

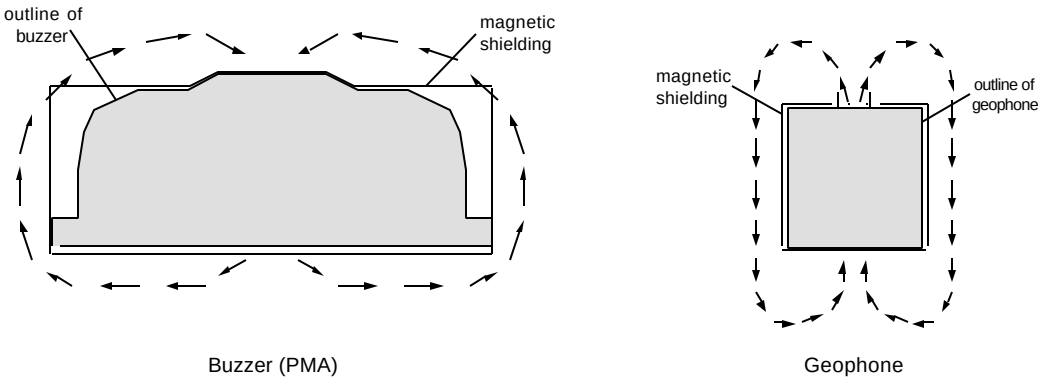


Figure 19: Stray magnetic fields from the PMAs and geophones

A detailed series of tests was conducted on the final HXA to characterize stray magnetic fields. At the locations of the two magnetometers, total DC fields were 4.3 μT, -3.3 μT, and 0.4 μT and –5.4 μT, -2.1 μT, and 4.5 μT in x, y, and z. These levels were significant but low enough so that the DC effect on the magnetometer readings could be calibrated out on the ground. AC measurements indicated negligible stray fields, under 0.5 μT in all axes at both magnetometers.

### 5.5 Temperature Sensor

The HXA includes one temperature sensor located in a recess in the x-y center of the base plate. The temperature will be recorded each time data is recorded by the DCS. For the HXA application the model AD590LH was used. The TO-52

package is mounted upside down in the top surface of the base plate and is held in place with a clamp. A two-wire connection to the AD590 is routed through the truth sensor wiring harness back to the DCS. A second AD590 sensor (model AD590MF) is located on the DCS circuit board. The 8-bit A/D converter limits the practical resolution of each measurement of temperature. The temperature is stored, and then displayed in the data viewing software in increments of 3.5 degrees Fahrenheit (1.94 °C).

### 5.6 Summary

This section has described in detail the various elements of the SUITE hexapod assembly (HXA). The HXA was integrated with the PICOSat spacecraft in June of 1998 and has subsequently been through spacecraft vibration qualification. A second, flight spare HXA is installed at the Air Force Research Lab. The flight spare is being used to test out vibration control algorithms prior to flight. In the short sections that follow, highlights of the data control system (DCS) are provided. These areas will be expanded on in separate papers describing the DCS and the vibration isolation control results.

## 6. ELECTRONIC SUBSYSTEMS – DATA CONTROL SYSTEM (DCS)

This section is an abbreviated summary of the data control system electronic hardware. The DCS is located in a 338 × 338 × 32 mm tall module tray in PICOSat and is separated from the HXA by another double-height tray. Three cable harnesses incorporating 78 individual wires connect the DCS and HXA. The DCS is functionally a single board computer, with processors, memory, power converters, programmable logic, a communications interface, and interfaces to the analog transducers of the HXA. The DCS receives +14V power from the host spacecraft, filters it for EMI, and converts it to +5V, ±15V, and +100 V. Total power draw for the DCS is approximately 0.9A at 14 V. At room temperature, the full SUITE system consumes 15-16 W in data acquisition mode, 16-18W in full control mode, and up to 22.5 W if a disturbance generator is being used to shake the spacecraft.

The heart of the DCS is a Texas Instruments TMS320C31 digital signal processor (DSP). The DSP runs on a 40 MHz clock. Two field programmable gate arrays (FPGAs) interface the DSP and memory with the rest of the DCS and the HXA. A PIC 16C74 microcontroller at 16 MHz performs several peripheral tasks, including communication with the PICOSat controller area network (CAN) bus, temperature sensor reads, and generation of PWM signals to drive the disturbance generators.

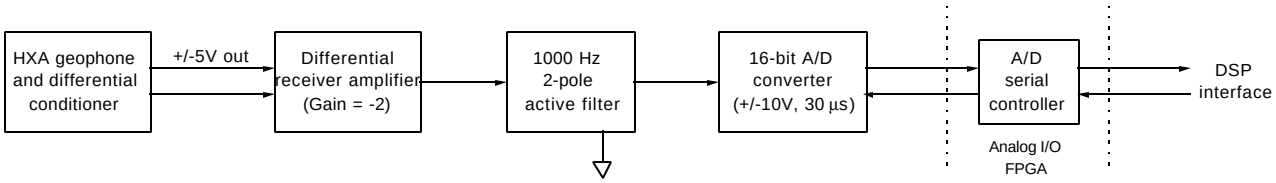


Figure 20: Input from geophone motion sensors to DSP

Figure 20 summarizes the flow of information in from the 12 motion sensors. The DCS has 12 independent 16-bit analog-to-digital converters. The lack of multiplexing is critical for fast multiple-channel control.

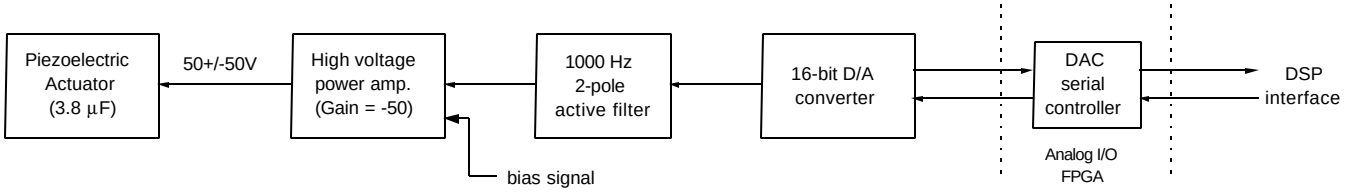


Figure 21: Output from DSP to piezoelectric actuators

Figure 21 summarizes the flow of information and signals from the DSP to the six piezoelectric actuators. Again, all six channels have independent DACs. The high voltage amplifier is a linear device operated well below its rated specifications.

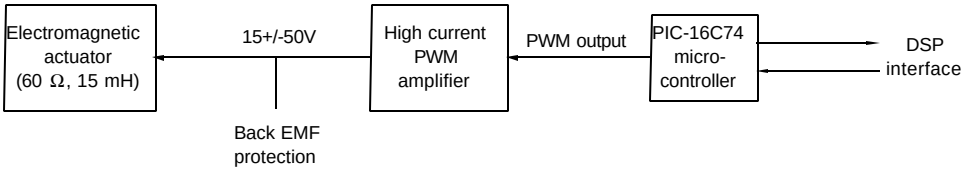


Figure 22: Output from DCS to disturbance generators

Figure 22 shows the system for generating and commanding the shakers of PMAs. The DSP creates 128-point tables of numbers, typically sinusoids, and these are placed in shared memory and access by the micrcontroller. From there, a PWM amplifier, using less than 20% of its capacity, drives the resistive/inductive loads.

## 7. SOFTWARE AND FIRMWARE

This section provides a brief summary of the SUITE software and firmware. The four major programmable parts on the DCS are the DSP, the microcontroller, and the two FPGAs. The DSP code is the most flexible in that it can be re-burned without any hardware modifications. This executive code was revised several times to accommodate unique features of the CAN interface and evolving requirements for control. New firmware can be burned using the Texas Instruments emulator interface or alternative interfaces such as Code Composer. New executive code cannot be re-burned remotely from the ground when PICOSat is in orbit.

The experiment code can be updated, and a once per week revision is planned. The process for developing this code is summarized in Figure 23. It begins and ends in MATLAB. The control code structure is flexible, but a baseline set of code has been established. This code accepts descriptions of state-space controllers through MATLAB-generated header files. With the three core control codes in place, the experiment lists allow selective running of numerous variations of the controllers. Thirty-two updateable parameters are allowed with each experiment. An assembly of experiments constitutes the list and the set of lists the mission. Data download is also programmed by means of experiment lists.

Data is received in binary file format, and then extracted into the custom MATLAB package EZSUITE™. This software checks the data for errors and then makes it available for time and frequency domain viewing and further processing. EZSUITE™ also tracks status of the DSP and microcontroller and extracts time and temperature references from the data.

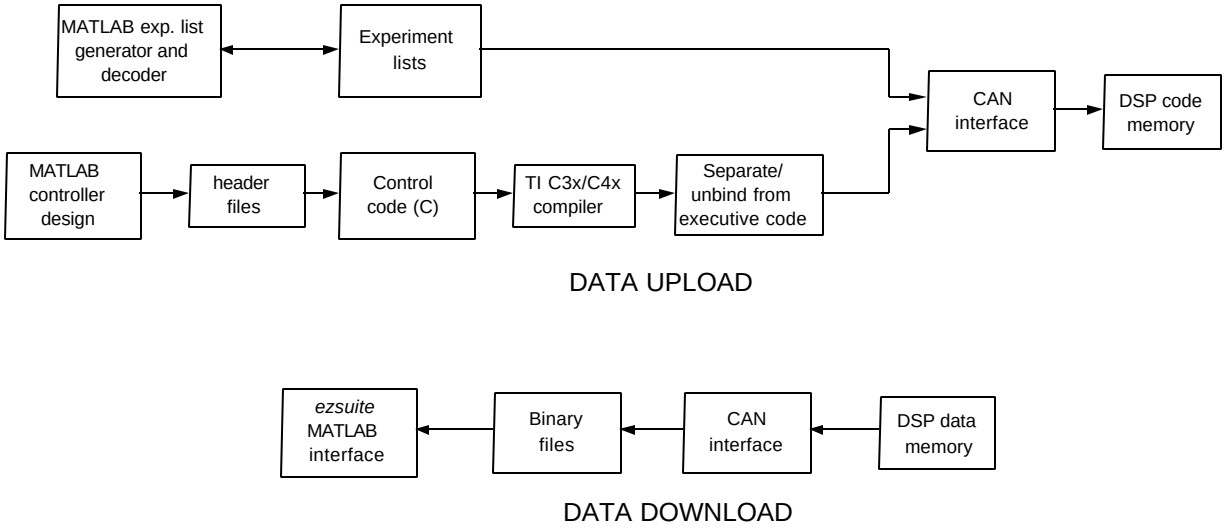


Figure 23: Flow of the SUITE code used to control the HXA

## 8. TEST RESULTS

Test results will be discussed in subsequent publications. One set of results is shown here. Figure 24 shows the measured transmissibilities of the HXA with the active control off. Measurements were done with an independent set of accelerometers. Note that in the radial direction, the system is softer, consistent with the predictions of Table 4. For reduced radial vibration transmission, the role of the active control is to reduce response in the 5 to 100 Hz range. The resonance at 300 Hz is a mode of the base plate resting on the test fixturing. The greater stiffness in the axial direction will require that the active control bandwidth extend to about 250 Hz to insure that the net transmissibility is below –20 dB.

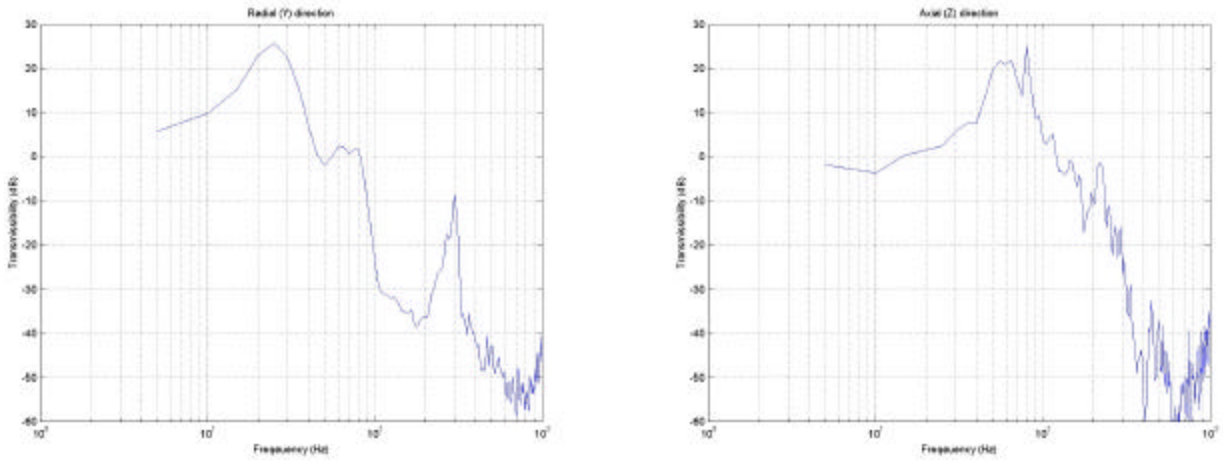


Figure 24: Measured transmissibilities using independent sensors for radial and axial directions of passively isolated hexapod

One final measurement is presented in Figure 25. SUITE functions as a spectrum analyzer in the internal acquisition of the 6×6 plant transfer function. Typically, a chirp input is used. The figure shows the transfer function matrix with the piezoelectric actuators driven and the geophone output signals measured. The main point of the figure is to demonstrate the similarity in the collocated transfer functions along the diagonal, and the reduced response in the off-diagonal directions. The diagonal dominance allows SISO control approaches to be relatively effective.

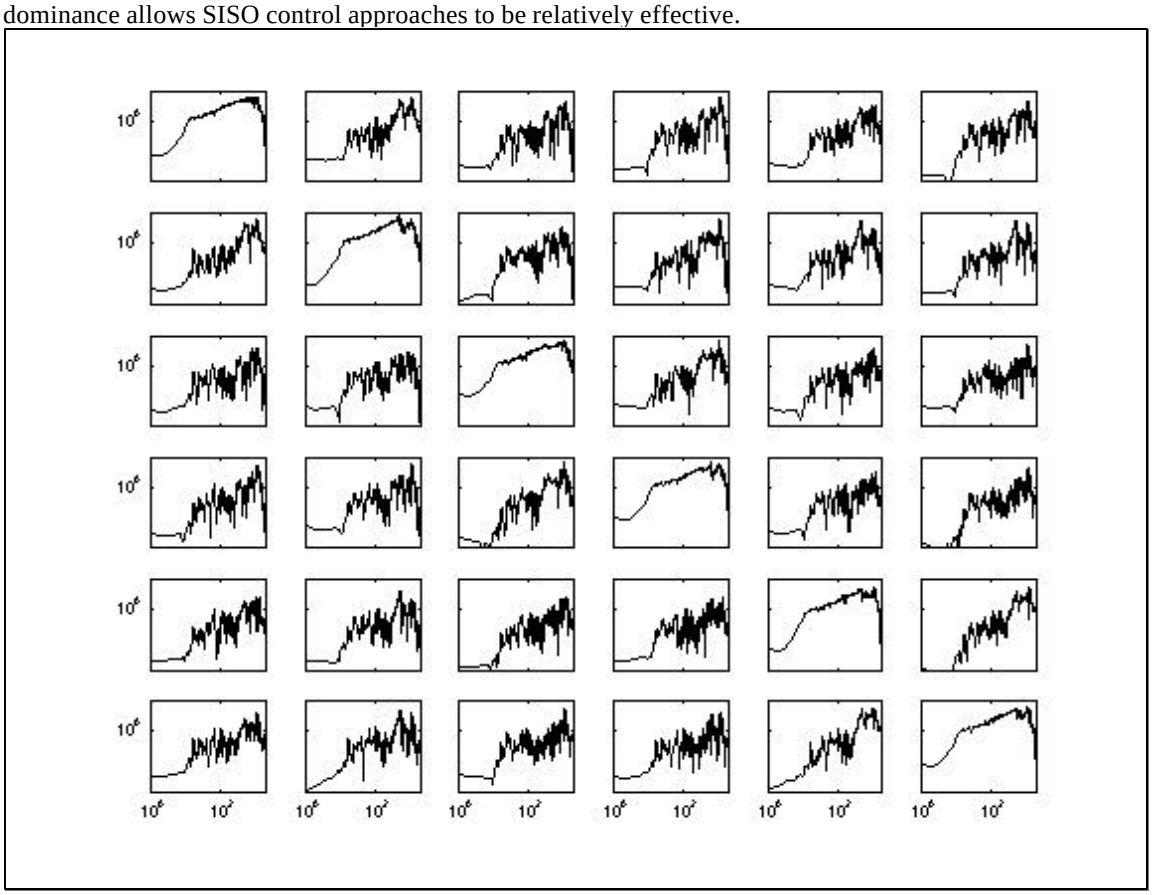

Figure 25: Open-loop plant transfer function showing decoupling between struts (1-2000 Hz, 0.001-30 V/V)

## CONCLUSIONS

This paper has described the Satellite Ultraquiet Isolation Technology Experiment (SUITE), emphasizing the electromechanical systems that make up the active hexapod assembly. The DSP-controlled piezoelectric-based active isolation system has been integrated with the PICOSat spacecraft and is planned to be launched as early as 2000. SUITE is a software-reconfigurable system that will serve as an on-orbit testbed for microprecision vibration control approaches for up to a year after its launch.

## ACKNOWLEDGEMENTS

This work was sponsored in part by the Air Force Research Laboratory under a Small Business Innovation Research Grant, contract number F29601-97-C-0025. The technical monitors for the contract were Captains Michelle Idle and Richard Cobb.

## REFERENCES

1. Anderson, E., Leo, D., and Holcomb, M., "Ultraquiet Platform for Active Vibration Isolation," Proc. SPIE Vol. 2717, p. 436-451, Smart Structures and Materials 1996: Smart Structures and Integrated Systems, Inderjit Chopra; Ed.
2. Glaser, R. J.; Garba, J. A.; and Obal, Michael, "STRV-1B Cryocooler Vibration Suppression," AIAA/ASME/ASCE/AHS/ASC, Structures, Structural Dynamics and Materials Conference, 36th, New Orleans, LA, Apr. 10-13, 1995; AIAA Paper 95-1122.
3. Bennett, S., Davis, T., Cobb, R., and Sullivan, J., *31st Aerospace Mecahnisms Symposium*, "Vibration Isolation, Steering, and Suppression for Space-based Sensors," NASA Marshall Space Flight Sensor, May, 1997.
4. Tobin, Maj. David M., Haag, Capt. Gary S., da Silva Curiel, Alex, Ward, Jeff, Allery, Mark, and Lorenzi, Jenny, "Off-the-Shelf MicroSatellites for Science and Technology Missions: The USAF PICOSat Mission Using the SSTL Modular Microsatellite," *11th AIA/USU Conference on Small Satellites*, Paper SSC97-V-4.
5. Riedesel, Mark A., Moore, Robert D., and Orcutt, John A., "Limits of Sensitivity of Inertial Seismometers with Velocity Transducers and Electronic Amplifiers," Bulletin of the Seismological Society of America, Vol. 80, No. 6, pp. 1725—1752, Dec. 1990.